ELSEVIER

Surface and Coatings Technology 128–129 (2000) 231–235

SURFACE & COATINGS TECHNOLOGY

www.elsevier.nl/locate/surfcoat

Macro-particle free metal plasma immersion ion implantation and/or deposition in a multifunctional configuration

T. Zhang[a,b], B.Y. Tang[a], Z.M. Zeng[a], Q.C. Chen[a], X.B. Tian[a], T.K. Kwok[a], P.K. Chu[a,*], O.R. Monteiro[c], I.G. Brown[c]

[a] *Department of Physics and Materials Science, City University of Hong Kong, 83 Tat Chee Ave., Kowloon, Hong Kong*
[b] *Institute of Low Energy Nuclear Physics, Beijing Radiation Center, Beijing Normal University, Beijing 100875, PR China*
[c] *Lawrence Berkeley National Laboratory, University of California, Berkeley, CA 94720, USA*

Abstract

For high-dose metal ion implantation, the use of plasma immersion offers the high-rate advantage, but the simultaneous formation of a surface film along with the sub-surface implanted layer is sometimes a detriment. In this work, we describe a metal plasma immersion approach in which pure and macro-particle free implantation (metal and/or gas ions), pure deposition without ion implantation, or dynamic metal ion beam assisted deposition and gaseous plasma immersion ion implantation (DIBAD metal and gas plasma immersion) can be obtained. We have demonstrated the technique by carrying out Ti and Ta implantation at approximately 80 keV (Ti) and 120 keV (Ta) and doses on the order of 1×10^{17} ions/cm^2. In our experiments, the Ta and Ti plasma immersion process can be tuned to give rise to implantation solely with no concomitant surface film formation. The atomic fraction of the applied dose that deposits as a film vs. the part that is energetically implanted during the DIBAD of metal and gas plasma immersion can be precisely controlled. This is a valuable method to fabricate advanced materials. © 2000 Elsevier Science S.A. All rights reserved.

Keywords: Metal plasma; Ion beam assisted deposition; Plasma immersion ion implantation

1. Introduction

A vacuum arc ion source provides a means to carry out metal ion implantation for the surface modification of metals, ceramics, semiconductors, superconductors, glass and polymers, and these are all active areas of ion implantation research. Due to its high metal ion flux, the vacuum arc ion source is widely used as a metal plasma source for film deposition as well. For example, DC vacuum arc sources and pulsed vacuum arc ion sources have been used to fabricate TiN and DLC (diamond like carbon) films [1–4]. Conventionally, a three-grid accelerator system is connected to the vacuum arc ion source for the purpose of metal ion implantation, but it tends to block the metal flux severely. As the experimental setups are quite different, film deposition and ion implantation are usually conducted separately. In addition, one ion source may not be able to perform optimally in the dynamic ion beam assisted deposition (DIBAD) process involving both ion implantation and deposition.

Recently, metal plasma immersion ion implantation and deposition have been developed [5–10]. A vacuum arc ion source is used to generate a metal beam with a high flux and charge state. When combined with gas plasma immersion ion implantation, DIBAD can be accomplished [11–13]. We have recently developed a practical, simple, and multi-functional DIBAD system. The triggering frequency of the metal arc source as well as the phase and duration of the negative high

* Corresponding author. Tel.: +852-2788-7724; fax: +852-2788-9549.
E-mail address: paul.chu@cityu.edu.hk (P.K. Chu).

0257-8972/00/$ - see front matter © 2000 Elsevier Science S.A. All rights reserved.
PII: S0257-8972(00)00653-8

voltage applied to the sample can be independently controlled. By the proper adjustment of the critical parameters, namely the duration and the phase of the metal plasma and high voltage bias pulses, the process can be fine tuned to achieve either pure implantation, pure deposition, or a hybrid process containing a variable ratio of implantation to deposition.

In this paper, we demonstrate the feasibility of the DIBAD approach and describe the plasma and high voltage experimental apparatus. Experimental results are acquired using Ti and Ta plasmas. It is shown that energetic, high-dose, macroparticle-free metal ion implantation can be accomplished in a relatively short time.

2. Experimental

The metal plasma was generated by a filtered vacuum arc plasma gun similar to the kind discussed by Boxman et al. [14] and Brown [15], and our particular equipment has been described [16]. The metal plasma source used a 1-cm diameter Ti or Ta cathode and a tungsten mesh anode positioned approximately 16 mm in front of the cathode. The plasma gun was located at the entrance of a 45° magnetic duct consisting of a vacuum elbow 8 cm in diameter and 50 cm long, about which a solenoid was wrapped to establish the duct magnetic field. The arc current pulse was 150 A and the duration was approximately 200 μs with a repetition rate of 33 pulses/s. The duct magnetic field was 320 G. An aluminum electrode (Bilek bias plate) was positioned at the duct wall and biased at approximately +15 V to enhance the plasma transport efficiency through the duct [17–19].

A plane collector plate to which samples were affixed was positioned approximately 15 cm from the duct exit in the vacuum chamber. Hence, the samples were positioned within the stream of filtered metal plasma transported via the duct into the main vacuum chamber. The plate with the silicon or stainless steel samples was connected to a high voltage, high current pulsing power supply. The pulse voltage could be varied from 0 to −40 kV and pulse width from 0 to 160 μs. The bias pulse was adjusted to be in phase with the timing of the plasma pulse at its arrival at the substrate location (Fig. 1). In the metal plasma immersion ion implantation work, the Ti and Ta implantation time was approximately 10 min. Because of the relatively slow rise and fall time of the plasma pulse, the 160-μs bias pulse enveloped most of the plasma pulse (Fig. 1c). The substrate pulse voltage and current were monitored. There was secondary electron suppression at the collector plate, and the monitored current was the sum of the bombarding ion current and the secondary electron

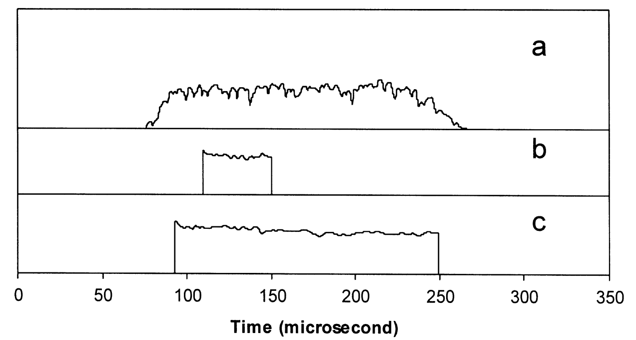

Fig. 1. Synchronization of the metal arc and sample high voltage pulse: The shape of the voltage pulses: (a) ion current waveform measured at the plane collector plate (sample) for one cathode arc pulse at a sample bias of −70 V. (b) High voltage waveform applied to the collector plate (sample) for both implantation and deposition (implantation when the sample voltage is on and deposition when the sample voltage is off). (c) High voltage waveform applied to the collector plate for pure implantation as the sample high voltage pulse width is almost the same as that of the cathodic arc.

current. We took the monitored current signal as only a semi-quantitative current indicator. In metal PIII and deposition, the chamber was filled with nitrogen to a pressure of 2×10^{-2} Pa. The nitrogen plasma was activated by a radio frequency (r.f.) source on top of the vacuum chamber. In the DIBAD experiments, the pulse width of the sample high voltage was 40 μs, and the entire pulse was enveloped by the metal flux pulse (Fig. 1b). When the sample high voltage was turned on, N and Ti ions were simultaneously implanted into the samples. When the high voltage was turned off, only Ti deposition occurred. The process time was 20 min.

The vacuum chamber base pressure was approximately 5×10^{-3} Pa (4×10^{-5} torr). In order to assess the efficacy of the duct to eliminate macro-particles produced in the cathodic arc, another set of Si wafers were deposited with Ti by positioning them in the duct 5 cm in front of the anode of the MEVVA source as well as in the chamber 15 cm from the outlet of the duct. A simplified schematic of the experimental configuration is exhibited in Fig. 2.

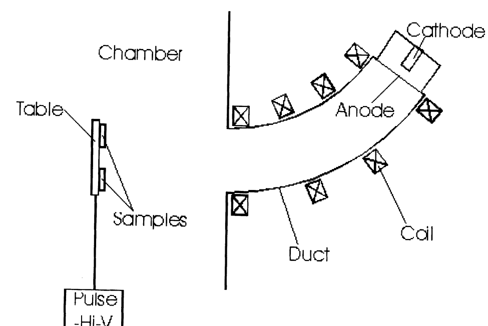

Fig. 2. Schematic of the metal plasma immersion ion implantation configuration.

3. Results and discussion

The implanted samples were characterized using 1.8 MeV helium ion Rutherford backscattering spectrometry (RBS), and the data were deconvoluted using the RUMP code. The Ta depth profile (40 kV implantation voltage) is depicted in Fig. 3a. For this sample, the calculated ion dose is 4.1×10^{16} ion/cm^2, and the measured range (depth of the peak) is approximately 240 Å. The Ti results are shown in Fig. 3b. Here, the dose is 7.9×10^{16} ions/cm^2 and the range is approximately 450 Å.

The metal plasmas formed in a vacuum arc discharge typically have ion charge states greater than unity. The charge state distributions of the ions in vacuum arc plasmas have been investigated [20], and it is known that under a wide range of conditions, the distributions remain basically constant. For the conditions of the present experiment, we can state that the charge state distribution for Ti is, within the uncertainty of the experiment, 11:75:14 for charge states $1+:2+:3+$, with a mean charge state of 2.1, and for Ta is 2:33:38:24:3 for charge states $1+:2+:3+:4+:5+$, with a mean charge state of 2.9. The fractional composition of the distribution is given in terms of particle current fractions, as is needed for consideration of implantation. Note that the particle current, i_p, is not the same as the electrical current, i_e, as measured by the Faraday cup, for example, and $i_p = i_e/Q$. The elevated ion charge states for Ti and Ta vacuum-arc-produced plasmas are significant in that the ion implantation energy is given by $E_i = QV_{bias}$. For a 40-kV bias voltage as used here, the mean implantation energies are, thus, approximately 84 keV for Ti and 116 keV for Ta.

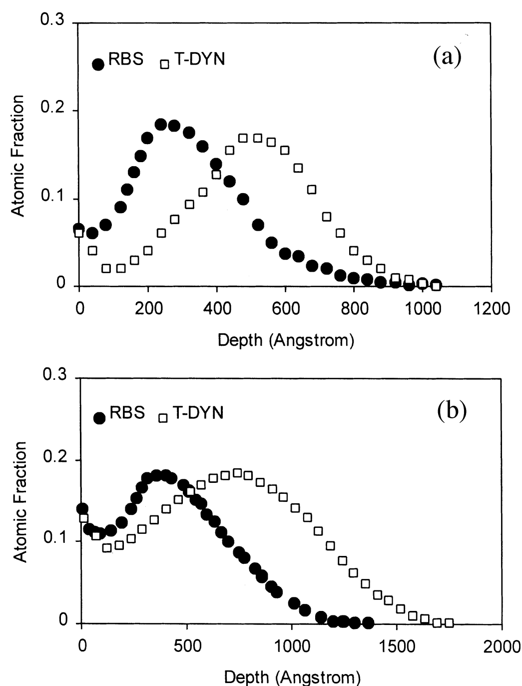

Fig. 3. Depth profiles derived from RBS data and computer simulation of the depth profiles by T-DYN: (a) Ta implanted into Si; (b) Ti implanted into Si. The ion energies used in computer calculation are 116 keV for Ta and 84 keV for Ti.

The RBS data can be compared with the results of a TRIM Monte-Carlo calculation [21] employing the actual ion energies involved. The TRIM-predicted ranges are 520 and 675 Å for Ta and Ti, respectively. We have also used the code T-DYN ('Dynamic TRIM') [22], which includes the effects of sputter erosion of the surface by the incident ions themselves. The calculated depth profiles for Ti and Ta ion implantation with energies of 84 and 116 keV and doses of 8×10^{16} and 4×10^{16}, respectively, are shown in Fig. 3a for Ta and Fig. 3b for Ti. As an approximation to incorporating the effects due to the different shapes of the plasma and high voltage pulses, we include in the simulation a correction factor that is based on previous work and accounts for the deposition (condensation of metal plasma on the substrate surface) of one ion per every 10 implanted ions. The T-DYN calculated ranges for these implantations agree well with the ranges calculated using TRIM. We, therefore, conclude that both TRIM and T-DYN, in the present application, provide good estimates of the Ti and Ta ranges expected, and that these values, approximately 650 and 500 Å, respectively, are greater than the RBS-measured depths. The primary reason for this discrepancy is believed to be due to sagging of the substrate bias voltage due to loading of the pulse generator by the high ion current. In fact, the measured profiles, especially for the Ti-implanted sample, have a shape would be expected for an implantation over a wide energy spread. This points out the necessity for a pulse generator possessing a high slew rate and high deliverable current for this application.

The DIBAD of Ti and N plasma immersion ion implantation is more difficult to conduct than Ti DIBAD or N PIII alone and requires careful synchronization of the individual processes. As shown in Fig. 4, the resulting film has an interlayer of approximately 400 Å. The broad interface is a manifestation of the ion mixing effects. Ti implantation has stronger mixing effects than that of N at the same acceleration voltage [23]. Our data show that Ti and N are evenly distributed in the film. Many factors influence the composition of the deposited film, such as the gas pressure, ionization ratio in the plasma, Ti ion flux intensity, and ratio of deposition-to-implantation. These parameters can be adjusted to cater for the process and the major factor determining the composition and quality of the films is the deposition-to-implantation ratio. Deposition only, that is, no implantation, usually results in poor adhesion between the film and substrate, but on

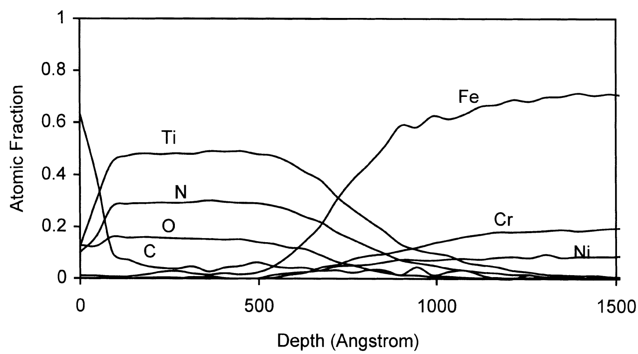

Fig. 4. Auger depth profile of the thin film fabricated on 304 stainless steel substrate using dynamic ion beam assisted deposition of Ti and N plasma immersion ion implantation. The metal pulse duration is 200 μs whereas the sample high voltage lasts for 40 μs.

the other hand, too much implantation gives rise to excessive sputtering thereby reducing the retained dose and film thickness. Thus, the deposition-to-implantation ratio must be optimally tuned. However, it should be noted that one can alter this ratio on the fly during the DIBAD/PIII experiment to achieve the desired film properties.

By turning off the sample high voltage while keeping the metal arc pulses on, a metal film can be deposited with no ion implantation effects. The scanning electron micrograph (SEM) of a Ti film deposited on the Si wafer positioned in the duct 5 cm in front of the anode, displayed in Fig. 5a, shows surface particles with size reaching 10–20 μm. This is typical of the macro-particles produced in a metal cathode arc. Therefore, a metal ion source without a filter to eliminate macro-particles may not yield desirable results [24–28]. On the contrary, the Ti film deposited on the Si wafer positioned in the chamber 15 cm from the outlet of the duct shows a macro-particle free SEM image (Fig. 5b), thereby demonstrating the high efficiency of the duct to filter these macro-particles. In a separate experiment, a 0.2-μm TiN film is fabricated using conditions similar to those described in the Ti DIBAD/N PIII experiments in the previous paragraph but without applying a high voltage to the sample. The TiN film on the Si wafer positioned in the duct 5 cm in front of the anode is coarse and tarnished. Point peeling can be visually spotted. The TiN film on the Si wafer positioned in the chamber 15 cm from the outlet of the duct, on the other hand, retains the shinny appearance, and no peeling can be observed. Our results unequivocally demonstrate that the filtered metal ion flux injected into the vacuum chamber is free of macro-particles.

4. Conclusion

The PIII configuration presented in this paper can perform multiple functions: pure implantation of metal ion; pure metal film deposition; a hybrid of dynamic surface film deposition and metal ion implantation; as well as gaseous ion or gaseous ion and metal ion PIII. The advantages are the high-rate, macro-particles free, and large area implantation capability, making the process suitable for not only non-semiconductor processes, but also semiconductor applications such as synthesis of buried conducting layers ($CoSi_x$, $IrSi_x$, etc.). Moreover, the process can synthesize surface and/or buried films containing different species. This is a valuable method to make advanced materials.

Acknowledgements

The work was supported by Hong Kong RGC Ear-

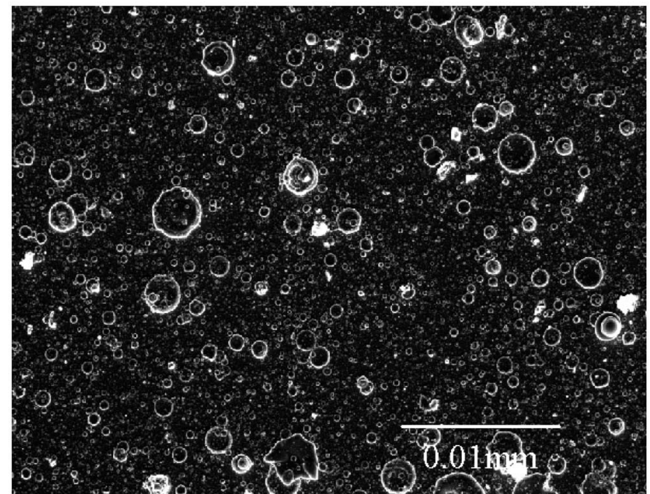

(a)

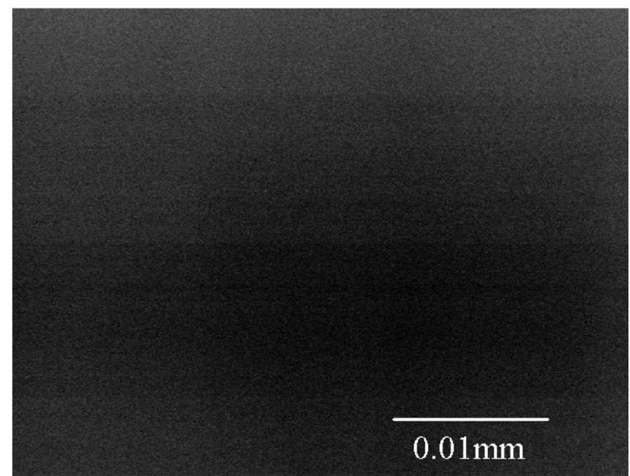

(b)

Fig. 5. SEM pictures of Ti films on Si: (a) sample located in the duct 5 cm in front of the anode showing macro-particles; (b) sample placed in the chamber 15 cm from the outlet of the duct.

marked Research Grants and #9040344 and 9040412 as well as the City University of Hong Kong Strategic Research Grant #7001028, as well as RGC/ Germany Joint Schemes 9050084 and 9050150. We also acknowledge K.M. Yu for the RBS analysis.

References

[1] P.J. Martin, A. Bendavid, T.J. Kinder, Proceedings of the Sixteenth International Symposium on Discharge and Insulation Vacuum, Berkeley, CA, 1996 p. 887.
[2] B.F. Coll, P. Sathrum, R. Aharonov, M.A. Tamor, Thin Solid Films 209 (1992) 165.
[3] R. Lossy, D.L. Pappas, R.A. Roy, J.J. Cuomo, V.M. Sura, Appl. Phys. Lett. 61 (1992) 171.
[4] P.J. Fallon, V.S. Veerasamy, C.A. Davis et al., Phys. Rev. B 48 (1993) 4777.
[5] I.G. Brown, X. Godechot, K.M. Yu, Appl. Phys. Lett. 58 (1991) 1392.
[6] I.G. Brown, A. Anders, S. Anders et al., Nucl. Instrum. Methods Phys. Res. B 80/81 (1993) 1281.
[7] A. Anders, S. Anders, I.G. Brown, M.R. Dickinson, R.A. MacGill, J. Vac. Sci. Technol. B 12 (1994) 815.
[8] O.R. Monteiro, Z. Wang, P.Y. Hou, I.G. Brown, Nucl. Instrum. Methods B 127/128 (1997) 821.
[9] O.R. Monteiro, Z. Wang, I.G. Brown, J. Mater. Res. 12 (1997) 2401.
[10] A. Anders, Surf. Coat. Technol. 93 (1997) 158.
[11] B.Y. Tang, P.K. Chu, S.Y. Wang, K.W. Chow, X.F. Wang, Surf. Coat. Technol. 103/104 (1998) 248.
[12] S.Y. Wang, P.K. Chu, B.Y. Tang, X.B. Tian, X.F. Wang, Q.Z. Lin, Thin Solid Films 311 (1997) 190.
[13] S.Y. Wang, P.K. Chu, B.Y. Tang, X.C. Zeng, X.F. Wang, Nucl. Instrum. Methods Phys. Res. B 127/128 (1997) 1000.
[14] R.L. Boxman, P.J. Martin, D.M. Sanders (Eds.), Vacuum Arc Science and Technology, Noyes, New York, 1995.
[15] I.G. Brown, Cathodic Arc Deposition of Films, in Annual Review of Materials Science, vol. 28, Annual Reviews Inc.,/ Palo Alto, CA, 1998.
[16] R.A. MacGill, M.R. Dickinson, A. Anders, O.R. Monteiro, I.G. Brown, Rev. Sci. Instrum. 69 (1998) 801.
[17] M.M.M. Bilek, D.R. McKenzie, Y. Yin, M. Chowalla, W.I. Milne, IEEE Trans. Plasma Sci. 24 (1996) 1291.
[18] M.M.M. Bilek, Y. Yin, D.R. McKenzie, IEEE Trans. Plasma Sci. 24 (1996) 1165.
[19] T. Zhang, B.Y. Tang, Z.M. Zheng et al., Rev. Sci. Instrum. 70 (8) (1999) 3329.
[20] I.G. Brown, X. Godechot, IEEE Trans. Plasma Sci. 19 (1991) 713.
[21] J.P. Biersack, S. Berg, C. Nender, Nucl. Instrum. Methods Phys. Res. B 59/60 (1991) 21.
[22] J.P. Biersack, Nucl. Instrum. Methods B 19/20 (1987) 32.
[23] G.Q. Li, T.C. Ma, T. Zhang, B.Y. Tang, P.K. Chu, Surf. Coat. Technol. 110 (1998) 1.
[24] S. Anders, A. Anders, K.M. Yu, X.Y. Yao, I.G. Brown, IEEE Trans. Plasma Sci. 21 (1993) 440.
[25] R.L. Boxman, S. Goldsmith, Surf. Coat. Technol. 43/44 (1990) 1024.
[26] K. Akari, H. Tamagaki, T. Kumakiri, K. Tsuji, Surf. Coat. Technol. 43/44 (1990) 312.
[27] J. Vyskocil, J. Musil, Surf. Coat. Technol. 43/44 (1990) 299.
[28] M. Ives, J.S. Brook, J. Cawley, W. Burgmer, Surf. Coat. Technol. 49 (1991) 244.